33rd International Cosmic Ray Conference, Rio de Janeiro 2013
The Astroparticle Physics Conference

ICRC 2013

Inner heliosphere spatial gradients of GCR protons in the low GeV range

Jan Gieseler[1], Mirko Boezio[2], Marco Casolino[3], Nicola De Simone[3], Valeria Di Felice[3], Bernd Heber[1], Matteo Martucci[3], Piergiorgio Picozza[3], and the PAMELA Collaboration.

[1] *Institute of Experimental and Applied Physics, University of Kiel*
[2] *INFN, Structure of Trieste and Physics Department of University of Trieste, Italy*
[3] *INFN, Structure of Rome "Tor Vergata" and Physics Department of University of Rome "Tor Vergata", Italy*

gieseler@physik.uni-kiel.de

Abstract: The spacecraft Ulysses was launched in October 1990 in the maximum phase of solar cycle 22, reached its final, highly inclined (80.2°) Keplerian orbit around the Sun in February 1992, and was finally switched off in June 2009. The Kiel Electron Telescope (KET) aboard Ulysses measures electrons from 3 MeV to a few GeV and protons and helium in the energy range from 6 MeV/nucleon to above 2 GeV/nucleon. Because the Ulysses measurements reflect not only the spatial but also the temporal variation of the energetic particle intensities, it is essential to know the intensity variations for a stationary observer in the heliosphere. This was accomplished in the past with the Interplanetary Monitoring Platform-J (IMP 8) until it was lost in 2006. Fortunately, the satellite-borne experiment PAMELA (Payload for Antimatter Matter Exploration and Light-nuclei Astrophysics) was launched in June 2006 and can be used as a reliable 1 AU baseline for measurements of the KET aboard Ulysses. Furthermore, we show that measurements of higher nuclei by the Advanced Composition Explorer (ACE), launched 1997 and still operating, can also be used as an extended baseline and to improve the analysis. With these tools at hand, we have the opportunity to determine the spatial gradients of galactic cosmic ray (GCR) protons between several tenth MeV to a few GeV in the inner heliosphere during the extended minimum of solar cycle 23.

Keywords: GCR, cosmic ray, gradient, Ulysses, PAMELA.

1 Introduction

Galactic cosmic rays (GCRs) enter the heliosphere isotropically and are exposed to multiple types of interactions as they traverse to the vicinity of the Earth, resulting in the so called modulation. The main effects are scattering at irregularities in the interplanetary magnetic field, gradient and curvature drifts, convection as well as adiabatic deceleration in the expanding solar wind. The importance of these particle drifts for the modulation of GCRs has been emphasized in the past [6]. Models including these effects [10] gave predictions for differently charged GCR particles which could be confirmed for both polarity solar cycles [1, 3, 7, 8]. Following these models, one expect the latitudinal gradient of positively charegd GCRs to be negative for an A<0 andpositive for an A>0 solar cycle, respecitvely, with an reversed behavior for electrons. The radial gradient should always be positive. Proton observations from Ulysses/KET have been used for such analysis in the past, using IMP 8 or ACE/CRIS as a 1 AU baseline [4, 5]. In a previous work we compared proton measurements of Ulysses/KET and PAMELA [2]. Here, we carry on with this analysis and investigate a broader energy range for protons.

2 Instrumentation

2.1 PAMELA

PAMELA (Payload for Antimatter Matter Exploration and Light-nuclei Astrophysics) is a satellite-borne spectrometer designed to study charged particles, in particular antiparticles, up to hundreds of GeV with high statistics and a sophisticated electron-proton discrimination. It was launched in June 2006 on an polar elliptical orbit around Earth with an altitude between 350 km and 600 km. During high latitude phases the low geomagnetic cutoff allows the detection of particles down to 50 MeV. A detailled description of the experiment can be found in [9].

2.2 Ulysses Kiel Electron Telescope

The Ulysses mission, launched 1990, delievered (amongst others) energetic particle measurements from February 1992 to June 2009 while on its highly inclined (80.2°) Keplerian orbit around the Sun. In particular, the Kiel Electron Telescope (KET) measured protons and α particles from 6 MeV/nucleon to above 2 GeV/nucleon and electrons from 3 MeV to a few GeV. See [12] for a full desciption of the instrument.

The trajectory information of Ulysses from 2006 to 2009 is shown in the lower panel of Fig.1. On top, the sunspot number and the tilt angle of the solar magnetic field are displayed, indicating that the investigation

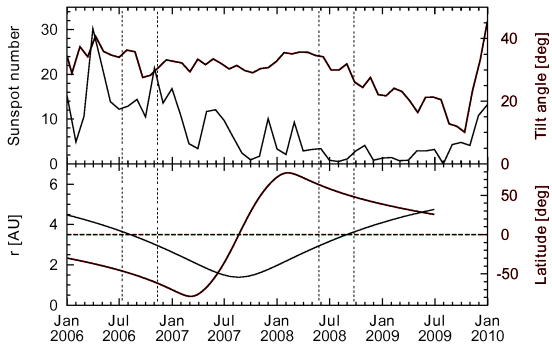

Figure 1: Time profiles of tilt angle, sunspot number (top), and Ulysses heliocentric latitude and radial distance (bottom). Shadings indicate the intervals used to investigate the temporal variation (see Sect. 3.2).

period showed very low solar activity, marking the unusual minimum of solar cycle 23. Two periods in late 2006 and mid 2008 are marked by shading when Ulysses was at nearly the same latitude and radial distance to the Sun. This has been used later for the analysis of the temporal variation.

3 Data Analysis

3.1 Mathematical Description of the Spatial Gradients

We assume that temporal and spatial variations of GCRs in the inner heliosphere can be separated [7]. It has been shown [1, 3, 7, 8] that the radial and latitudinal gradients G_r and G_θ are rigidity dependent. Thus, we compare the GCR intensities J at rigidity R and time t averaged over one solar rotation. Let $J_U(R,t,r,\theta)$ and $J_E(R,t,r_E,\theta_E)$ be the intensities measured by Ulysses/KET on its orbit and PAMELA at Earth, respectively. These intensities can be connected (at the same rigidity) with a function $f(R,\Delta r,\Delta\theta)$ that depends on the differences in heliospheric radial distance ($\Delta r = r_U - r_E$) and latitude ($\Delta\theta = |\theta_U| - |\theta_E|$) between the two observers:

$$J_U(R,t,r,\theta) = J_E(R,t,r_E,\theta_E)\cdot f(R,\Delta r,\Delta\theta) \quad (1)$$

Here, we assume a symmetric distribution of GCRs with respect to the heliographic equator, although small asymmetries have been found in the past [4, 13]. If we further make the assumption that the variations in radius and latitude are separable and can be approximated by an exponential law, Eq. 1 can be rewritten as:

$$J_U(R,t,r,\theta) = J_E(R,t,r_E,\theta_E)\cdot e^{G_r\Delta r}\cdot e^{G_\theta\Delta\theta} \quad (2)$$

with the rigidity dependent radial and latitudinal gradients G_r and G_θ.

3.2 Selection of Comparison Channels

To make sure that we compare measurements at the same rigidity, we apply the same method as in our previous analysis [2]. We use the high rigidity resolution of PAMELA as a calibration tool for the rigidity dependent geometric factors of the Ulysses/KET protons.

Channel	<E_{KET}>/GeV	<E_{PAM}>/GeV
P190.1	0.527	0.517
P190.2	0.945	0.923
P190.3	1.182	1.133

Table 1: Mean energies of selected proton measurement channel pairs of Ulysses/KET and PAMELA for which the gradients are individually calculated.

Marked by shading in Fig. 1 are the two time periods t_1 (July 2006 to November 2006) and t_2 (May 2008 to September 2008) when Ulysses was at almost the same position in the southern and northern solar hemisphere, respectively, so that $r_1 \approx r_2$ and $|\theta_1| \approx |\theta_2|$. Under the assumption that the spatial gradients do not change between t_1 and t_2, it follows that the arguments of the exponential functions from Eq. 2 are the same for both periods and the effects of spatial gradients cancel out. Thus, we can directly compare the ratios of the intensity measurements of Ulysses/KET and PAMELA of both periods:

$$\frac{J_U(R,t_1,r_1,\theta_1)}{J_U(R,t_2,r_2,\theta_2)} = \frac{J_E(R,t_1,r_E,\theta_E)}{J_E(R,t_2,r_E,\theta_E)} \quad (3)$$

The resulting time variations are shown in Fig. 2. They are plotted with respect to energy (instead of rigidity) to allow an easier differentiation between observations of protons and heavier ions. As expected, the modulation is higher at lower energies and vanishes for high energies. We can now verify that selected measurement channels of PAMELA are sensitive to the same energetic particle populations as Ulysses/KET because they show (within error limits) the same temporal variation. Since our previous work [2], the PAMELA proton data has been further investigated and refined. This process has not been finished yet for α particles. Thus, their analysis will be the topic of a future effort. For now, we end up with a selection of three proton channel pairs of Ulysses/KET and PAMELA measurements for which we individually determine the spatial gradients (cf. Tab. 1). In addition, Fig. 2 demonstrates that in principle we can use ACE/CRIS measurements of higher nuclei at Earth as a 1 AU baseline to calculate the spatial gradients of α particles detected at the Ulysses orbit. This will be done in an upcoming work.

3.3 Calculation of the Spatial Gradients

To calculate the radial and latitudinal gradients G_r and G_θ, we can rewrite Eq. 2:

$$\ln\left[\frac{J_U}{J_E}\right] = G_r\cdot\Delta r + G_\theta\cdot\Delta\theta \quad (4)$$

$$\underbrace{\frac{1}{\Delta r}\ln\left[\frac{J_U}{J_E}\right]}_{=:Y} = G_r + G_\theta\cdot\underbrace{\frac{\Delta\theta}{\Delta r}}_{=:X} \quad (5)$$

$$Y = G_r + G_\theta\cdot X \quad (6)$$

Under the assumption that the gradients are independent of time and space, they can easily be obtained by the slope and offset of a straight line which is fitted

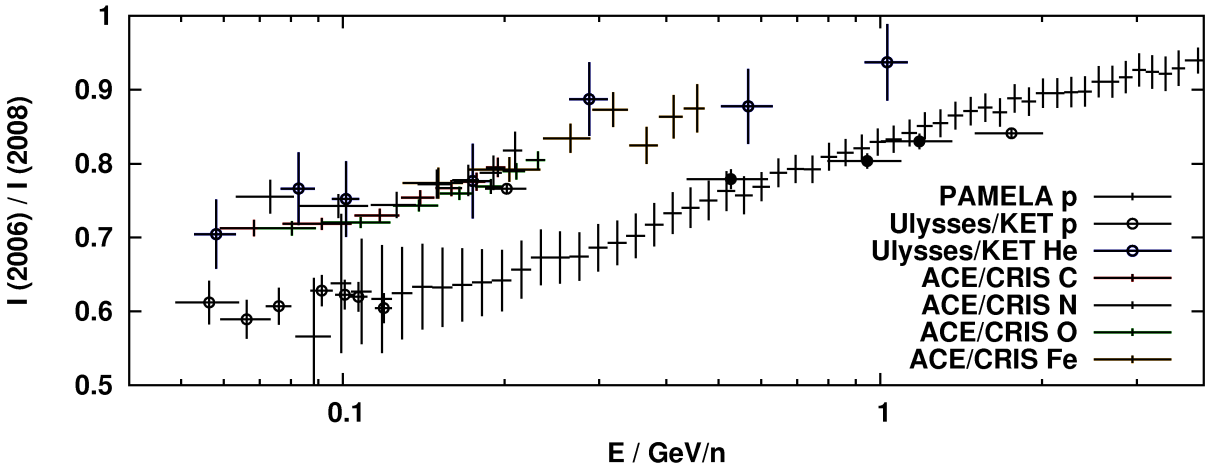

Figure 2: Time variations from 2006 to 2008 of different particle intensity measurements with respect to energy. Marked by full circles are the Ulysses/KET proton channels used here for gradient calculations.

	all data		without FLS		slow ascent (green)		slow descent (blue)	
	Fit (1)	Fit (2)	Fit (1)	Fit (2)	Fit (1)	Fit (2)	Fit (1)	Fit (2)
P190.1								
G_r	2.24±0.36	2.97±0.2	3.24±0.13	2.87±0.2	4.84±0.34	5.08±0.6	2.23±0.15	2.17±0.24
G_θ	-0.054 ±0.01	-0.044 ±0.007	-0.054 ±0.005	-0.036 ±0.007	-0.063 ±0.01	-0.073 ±0.019	-0.036 ±0.006	-0.036 ±0.011
χ^2/ndf	7.024	5.476	5.311	5.095	2.034	1.994	4.811	4.841
P190.2								
G_r	2.48±0.2	3.01±0.16	3.08±0.1	2.99±0.16	2.19±0.25	2.19±0.42	3.13±0.12	3.15±0.19
G_θ	-0.043 ±0.006	-0.055 ±0.006	-0.050 ±0.004	-0.053 ±0.006	-0.040 ±0.008	-0.041 ±0.013	-0.031 ±0.006	-0.036 ±0.009
χ^2/ndf	5.207	4.884	5.52	5.428	4.262	4.259	6.1	6.075
P190.3								
G_r	2.14±0.21	2.51±0.16	2.67±0.11	2.47±0.16	1.85±0.28	2.22±0.44	2.39±0.11	2.22±0.18
G_θ	-0.063 ±0.006	-0.069 ±0.006	-0.066 ±0.005	-0.066 ±0.006	-0.059 ±0.009	-0.07 ±0.014	-0.039 ±0.005	-0.036 ±0.009
χ^2/ndf	4.25	4.033	4.619	4.497	4.493	4.413	4.679	4.622

Table 2: Radial and latitudinal gradients (in %/AU and %/degree, respectively) and quality of fit for different selection criteria (cf. Fig. 3) and fit methods. Indicated by (1) are the values obtained by the bootstrap Monte-Carlo approach while (2) marks the fit routine using the `fitexy` algorithm. See Tab. 1 for corresponding energies.

through the data of a graph where $Y = \ln[J_U/J_E]/\Delta r$ is plotted over $X = \Delta\theta/\Delta r$. This is shown for one selected pair of Ulysses/KET and PAMELA measurements in Fig. 5. In addition, Fig. 3 and 4 show the orbit data (Δr and $\Delta\theta$) and the corresponding intensity ratio J_U/J_E, respectively. In all of these three Figures three different phases of the Ulysses trajectory are color coded: Red indicates the fast latitude scan (FLS) while the slow ascent and descent in both solar hemispheres are marked in green and blue, respectively.

In order to include the uncertainties of Fig. 5 in the fit calculation, two different methods are applied:

Minimization of the sum of squares, using the definition of χ^2 from the `fitexy` function from Numerical Recipes [11] to fit the data with errors in both x and y dimension.

Bootstrap Monte-Carlo approach. We choose for each data point randomly a value inside of its uncertainties, and calculate the fit for this ensemble of data points. This process is repeated 100 000 times. Our final values for the gradients are then the mean values over these 100 000 iterations, with the standard deviations as their error.

Because Ulysses covers such a wide latitude range during the FLS, the uncertainties in X are quite large in this interval. Therefore, the gradient calculation is carried out using the data from all times, without the FLS, and from the slow ascent and descent only, respectively. The results are shown in Tab. 2 and Fig. 6.

4 Summary and Conclusion

We investigated the spatial gradients of ~0.1-1.2 GeV GCR protons in the inner heliosphere from 2006 to 2009, during the unusual solar minimum of solar

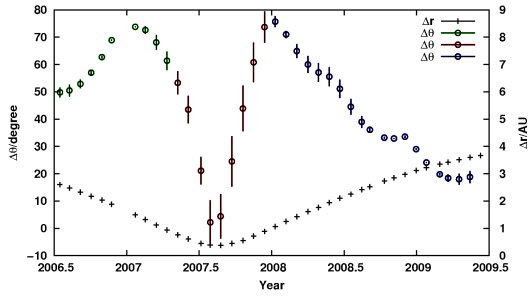

Figure 3: Differences in radial and latitudinal distance (Δr and $\Delta\theta$) between Ulysses and PAMELA for the analysis period. Marked in red is the fast latitude scan (FLS) of Ulysses while green and blue indicate its slow ascent and descent, respectively.

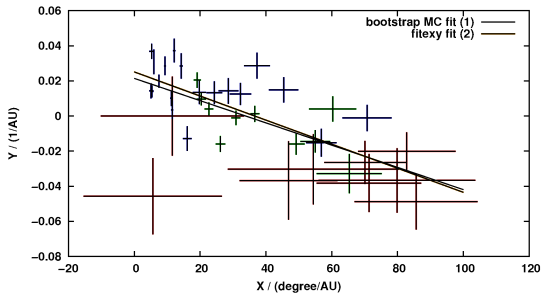

Figure 5: Y as a function of X (cf. Eq. 5) for P190.3. See Fig. 3 for color coding. The lines show the results of the two different fit methods, with $G_r = (2.14 \pm 0.21)\%/\mathrm{AU}$ and $G_\theta = (-0.063 \pm 0.006)\%/\mathrm{deg}$ for the bootstrap Monte-Carlo approach (black), and $G_r = (2.51 \pm 0.16)\%/\mathrm{AU}$ and $G_\theta = (-0.069 \pm 0.006)\%/\mathrm{deg}$ for the fit routine using the `fitexy` algorithm (orange).

cycle 23 (A<0). As expected, the radial gradients are always positive. They are also in the same range as in our previous analysis [2], the small differences can be attributed to a slightly changed analysis method and the already mentioned PAMELA data refinement. Nevertheless, our radial gradients are smaller than previous results [7]. In agreement with the expectations is the fact that our latitudinal gradients are small and negative. But they are by a factor of ∼2 bigger than previously [2]. This shows how sensitive the analysis is to small changes in the data. However, our findings are still almost zero and with that smaller than predicted by previous A<0-solar magnetic epoch observations [1, 7] and simulations [10].

Acknowledgment: The Ulysses/KET project is supported under Grant 50 OC 1302 by the German Bundesministerium für Wirtschaft through the Deutsches Zentrum für Luft- und Raumfahrt.The PAMELA mission is sponsored by the Italian National Institute of Nuclear Physics (INFN), the Italian Space Agency (ASI), the Russian Space Agency (Roskosmos), the Russian Academy of Science, the Deutsches Zentrum für Luft- und Raumfahrt (DLR), the Swedish National Space Board (SNSB) and the Swedish Research Council (VR). The German-Italian collaboration has been supported by the Deutsche Forschungsgemeinschaft under grant HE3279/11-1. Sunspot number data was obtained via the web site http://sidc.be/sunspot-data/ courtesy of the SIDC-team, Royal Observatory of Belgium. Wilcox Solar Observatory data was obtained via the web site http://wso.stanford.edu courtesy of J.T. Hoeksema.

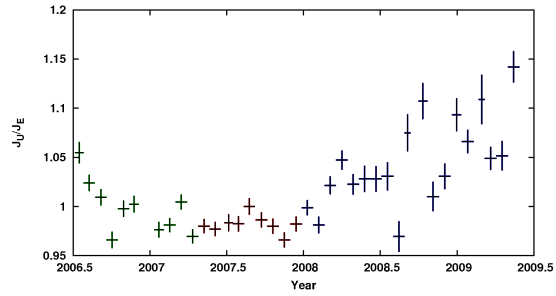

Figure 4: Intensity ratio time profile of P190.3 (cf. Tab. 1). See Fig. 3 for color coding.

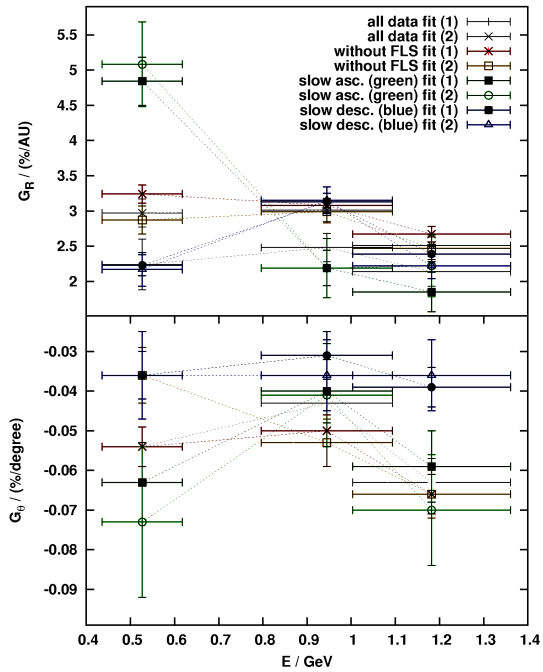

Figure 6: Radial and latitudinal gradients for different selection criteria and fit methods, as in Tab. 2.

References

[1] Cummings, A.C. et al. 1987, Geophys. Res. Lett., 14, 174
[2] De Simone, N. et al. 2011, Astrophys. Space Sci. Trans., 7, 425
[3] Heber, B. et al. 1996, Astron. Astrophys., 316, 538
[4] Heber, B. et al. 1996, Geophys. Res. Lett., 23, 1513
[5] Heber, B. et al. 2008, Astrophys. J., 689(2), 1443
[6] Jokipii, J.R. et al. 1977, Astrophys. J., 213, 861
[7] McDonald, F.B. et al. 1997, J. Geophys. Res., 102, 4643
[8] McKibben, R.B. 1989, J. Geophys. Res., 94, 17021
[9] Picozza, P. et al. 2007, Astropart. Phys., 27(4), 296
[10] Potgieter, M.S. et al. 2001, Adv. Space Res., 27, 481
[11] Press, W.H. et al. 1996, Numerical Recipes in Fortran
[12] Simpson, J.A. et al. 1992, Astron. Astrophys. Suppl., 92, 365
[13] Simpson, J.A. et al. 1996, Astrophys. J. Lett., 465, L69